

## High-Voltage, Pulsed Electric Fields Eliminate *Pseudomonas aeruginosa* Stable Infection in a Mouse Burn Model

Mengjie Wu,<sup>1,2</sup> Andrey Ethan Rubin,<sup>3</sup> Tianhong Dai,<sup>4,5</sup> Rene Schloss,<sup>6</sup> Osman Berk Usta,<sup>2</sup> Alexander Golberg,<sup>3,†</sup> and Martin Yarmush<sup>2,6,7,\*,†</sup>

<sup>1</sup>Department of Orthodontics, The Affiliated Stomatology Hospital, Zhejiang University School of Medicine, Hangzhou, China.

<sup>2</sup>Center of Engineering in Medicine; <sup>4</sup>Wellman Center for Photomedicine; <sup>5</sup>Vaccine and Immunotherapy Center; Massachusetts General Hospital, Harvard Medical School, Boston, Massachusetts, USA.

<sup>3</sup>Porter School of Environment and Earth Sciences, Tel Aviv University, Tel Aviv, Israel.

<sup>6</sup>Department of Biomedical Engineering, Rutgers University, Piscataway, New Jersey, USA.

<sup>7</sup>Shriners Burn Hospital for Children, Boston, Massachusetts, USA.

<sup>†</sup>These two authors contributed equally to this work.

**Objective:** The incidence of severe infectious complications after burn injury increases mortality by 40%. However, traditional approaches for managing burn infections are not always effective. High-voltage, pulsed electric field (PEF) treatment shortly after a burn injury has demonstrated an antimicrobial effect *in vivo*; however, the working parameters and long-term effects of PEF treatment have not yet been investigated.

**Approach:** Nine sets of PEF parameters were investigated to optimize the applied voltage, pulse duration, and frequency or pulse repetition for disinfection of *Pseudomonas aeruginosa* infection in a stable mouse burn wound model. The bacterial load after PEF administration was monitored for 3 days through bioluminescence imaging. Histological assessments and inflammation response analyses were performed at 1 and 24 h after the therapy.

**Results:** Among all tested PEF parameters, the best disinfection efficacy of *P. aeruginosa* infection was achieved with a combination of 500 V, 100  $\mu$ s, and 200 pulses delivered at 3 Hz through two plate electrodes positioned 1 mm apart for up to 3 days after the injury. Histological examinations revealed fewer inflammatory signs in PEF-treated wounds compared with untreated infected burns. Moreover, the expression levels of multiple inflammatory-related cytokines (interleukin [IL]-1 $\alpha/\beta$ , IL-6, IL-10, leukemia inhibitory factor [LIF], and tumor necrosis factor-alpha [TNF- $\alpha$ ]), chemokines (macrophage inflammatory protein [MIP]-1 $\alpha/\beta$  and monocyte chemoattractant protein-1 [MCP-1]), and inflammation-related factors (vascular endothelial growth factor [VEGF], macrophage colony-stimulating factor [M-CSF], and granulocyte-macrophage colony-stimulating factor [G-CSF]) were significantly decreased in the infected burn wound after PEF treatment.

**Innovation:** We showed that PEF treatment on infected wounds reduces the *P. aeruginosa* load and modulates inflammatory responses.

**Conclusion:** The data presented in this study suggest that PEF treatment is a potent candidate for antimicrobial therapy for *P. aeruginosa* burn infections.

**Keywords:** burn infection, pulsed electric field, inflammation, disinfection



Alexander Golberg, PhD,  
and Martin Yarmush, MD, PhD

Submitted for publication December 22, 2019. Accepted in revised form October 12, 2020.

\*Correspondence: Alexander Golberg, Porter School of Environment and Earth Sciences, Tel Aviv University, Tel Aviv 69978, Israel (email: agolberg@tauex.tau.ac.il); or Martin Yarmush, Department of Biomedical Engineering, Rutgers University, Piscataway, NJ, 08854, USA (email: ireis@sbi.org).

## INTRODUCTION

BURN INJURY IS one of the most common and devastating causes of trauma in global public health, with ~14,000 burn patients reported annually in the United States.<sup>1,2</sup> Burn injury is always accompanied by local or systemic infections that lead to various pathological events, such as extreme toxicity, high fever, hyperdynamic circulation, bacteremia, hypotension, and cardiovascular collapse,<sup>3</sup> which may subsequently contribute to increased incidence of sepsis, organ failure, and death.<sup>4</sup> Gram-negative bacteria are the predominant causative agents and etiologic factors of burn infection,<sup>5</sup> with *Pseudomonas aeruginosa* being the most common pathogen.<sup>6</sup> According to swab tests and tissue culture, the rate of *P. aeruginosa* infections is as high as 57% in all burn infection cases.<sup>7</sup> Moreover, *P. aeruginosa* may also cause significant hospital-associated outbreaks in wounds, particularly due to the emergence of many multidrug-resistant strains.<sup>8,9</sup>

The clinical management of burn therapy has multilevel goals, ranging from reducing pain, facilitating healing, and minimizing scarring to achieving recovery of normal functions.<sup>10</sup> Multidisciplinary commitment is required in controlling burn infections, which includes the application of topical and systemic antimicrobials associated with an antimicrobial stewardship principle.<sup>11</sup> The development of antimicrobial resistance has several risk factors associated with the severity of infections, and antimicrobial resistance itself is associated with increased mortality.<sup>12</sup> Antimicrobial resistance has led to a major restriction in the treatment options of *P. aeruginosa* infections, which has become a critical and deadly issue.<sup>13</sup> Therefore, there is a great need for alternative nonpharmacological approaches in the clinical manipulation of burn wounds.<sup>14,15</sup>

Chemical-free nonthermal techniques are promising novel methods for bacterial disinfection. In particular, electroporation is an attractive approach for various cell therapies.<sup>16</sup> Electroporation is a process that increases cell membrane permeability to ions and macromolecules by exposing the cell to a short, high-voltage, pulsed electric field (PEF).<sup>17</sup> Electroporation can be categorized into two types: reversible electroporation is commonly used to deliver DNA into cells, whereas irreversible electroporation is used for direct nonthermal ablation of solid tumors.<sup>18</sup> The vulnerability of cells to electroporation treatment is based on their surface charge, external environmental temperature, membrane composition, and pH value.<sup>19</sup> Noticeably, the effects of high-voltage, monophasic, pulsed elec-

trical current on inhibiting bacterial burden and/or healing of chronic wounds in patients have recently been reported.<sup>20–22</sup> However, the uncertainty of pulse parameter selection, which directly links electroporation efficiency and bactericidal effects, hampers the widespread adoption of PEF-mediated wound sterilization in burn wound treatment.<sup>23,24</sup> In addition, little is known regarding how PEF treatment affects *P. aeruginosa* infection and related immune responses in burn injuries.<sup>25</sup> Therefore, the goal of the present study was to optimize the working parameters of PEF treatment for burn wound *P. aeruginosa* disinfection and to evaluate the inflammatory response after PEF treatment of the infected wound.

## CLINICAL PROBLEM ADDRESSED

The incidence of severe infectious complications after burn injury increases mortality by 40%.<sup>9</sup> Thus, successful treatments of infections and septic episodes are of great importance to decrease the mortality due to severe burn injury.<sup>26</sup> Traditional approaches for management of burn infection include early surgical debridement, skin grafting, and the use of topical and prophylactic antibiotics, which are not always effective.<sup>14</sup> To address these problems, we propose the use of nonthermal, high-voltage PEF technology to facilitate disinfection and healing of burn wounds, which has previously been shown to be effective for treating wounds and surgical mesh infection.<sup>27,28</sup> PEF treatment has been suggested to directly kill bacterial cells by the irreversible electroporation of cell membranes; however, only a few studies have examined its direct effect on bacterial infection. Furthermore, to better understand the therapeutic mechanism and ensure host safety, the immunological response to PEF treatment of burn infections is of high clinical relevance and should be investigated.

## MATERIALS AND METHODS

### Animals

Seven- to 8-week-old female BALB/c mice weighing 17 to 21 g were purchased from Charles River Laboratories (Wilmington, MA). The animals were housed in cages with access to food and water *ad libitum* and maintained on a 12-h light–12-h dark cycle at a room temperature of ~21°C and relative humidity of 30–70%. All animal procedures were approved by the Institutional Animal Care and Use Committee (IACUC) of Massachusetts General Hospital and the guidelines of the National Institutes of Health (NIH) were followed.

Two sets of animal experiments were performed. First, we optimized the PEF parameters using 11 groups of mice ( $N=3$  per group). After the optimization experiments were completed, an additional six animals were used to study 1-h and 24-h effects of optimized PEF parameters. At each time point, three tissue samples were used for qualitative histological assessments and six animal tissue samples were used to quantify the levels of cytokines, chemokines, and growth factors.

#### ***P. aeruginosa* strain and culture conditions**

A bioluminescent variant of the *P. aeruginosa* strain PA-O1 (PA-O1: *lux*) that contains an integrated *lux* operon from *Photobacterium luminescens* was a kind gift from Dr. Joanna B. Goldberg at the Emory University School of Medicine. PA-O1 is an opportunistic pathogen that causes serious infection in immunocompromised hosts, and the use of the PA-O1: *lux* strain allows for real-time monitoring of bioluminescence from bacterial cells.<sup>29</sup> The bacteria were grown in a brain heart infusion medium supplemented with 50  $\mu\text{g}/\text{mL}$  kanamycin in an orbital incubator (37°C, 100 rpm) overnight. Subsequently, the cells were centrifuged, washed with phosphate-buffered saline (PBS), and resuspended in PBS to an optical density of 0.6–0.8 at 600 nm, which corresponds to  $\sim 10^8$  CFU/mL.

#### ***P. aeruginosa* burn infection in mice**

The stable burn infection in the mouse model was done as described in detail previously (Supplementary Figs. S1 and S2).<sup>30</sup> Briefly, before administering a burn wound, mice were anesthetized by intraperitoneal (i.p.) injection of a ketamine–xylazine cocktail, shaved on the dorsal surfaces, and treated with depilatory cream (Sally Hansen® Div. Del Laboratories, Farmingdale, NY). A pre-heated (in boiling water,  $\approx 95^\circ\text{C}$ ), cubic brass block ( $\sim 8.6$  g) was applied (1.22 psi), without any exter-

nal pressure, on the dorsal surface of each mouse for 7 s, resulting in a third-degree thermal burn with a surface area of  $\sim 1\text{ cm}^2$  (Supplementary Fig. S3). Then, 5 min after burning, 50  $\mu\text{L}$  of a bacterial suspension containing  $10^8$  CFU/mL was topically applied using a syringe to the eschar of each burn. Buprenorphine was administered to the mice as a painkiller before and after burning on the first day and then twice a day for the following 3 days.

#### **Optimization of parameters for PEF treatment**

PEF treatment was applied 24 h after infection with PA-O1: *lux*, as previously described.<sup>31</sup> Before PEF treatment, animals were anesthetized with isoflurane. Then, their fur was clipped along the dorsal surfaces, and a designated area was subjected to electroporation using contact electrodes. Thirty-three mice were randomly divided into 11 groups ( $N=3$  per group) and subjected to PEFs with different parameters (Table 1). Square pulses<sup>32</sup> were delivered using a BTX 830 pulse generator (Harvard Apparatus, Holliston, MA). Food intake was monitored every day after the PEF treatment.

#### **Bioluminescence imaging**

It has been well documented that the bacterial luminescence signal is correlated with bacterial viability in real time.<sup>29,33</sup> The loss of bacterial luminescence indicates the loss of bacterial viability.<sup>29,33</sup> Thus, the use of a luminescent *P. aeruginosa* strain (PAO1: *lux*) allows for the daily quantitative assessment of bacterial burden for *P. aeruginosa* wound infections. Before imaging, the mice were anesthetized by i.p. injections of a ketamine–xylazine cocktail. The mice were then placed on an adjustable stage in a specimen chamber, and the infected burns were positioned directly under an IVIS Lumina (series III) camera

**Table 1.** Experimental design for high-voltage, pulsed electric field parameter optimization for PA-O1: *lux* disinfection in burn wounds

Group No.	Voltage, V	Pulse duration, $\mu\text{s}$	Number of pulses	Current, A <sup>a</sup>	$\mu\text{C}/\text{s}$	C/treatment duration
1 Blank control: uninfected wounds	0	0	0	0	0	0
2 Burn injury with infection, w/o PEF (negative control)	0	0	0	0	0	0
3	500	200	80	3.1	0.116	0.050
4	500	200	100	3.1	0.093	0.062
5	500	200	120	3.1	0.078	0.074
6	500	200	160	3.1	0.058	0.099
7	500	200	180	3.1	0.052	0.112
8	500	100	200	3.1	0.047	0.062
9	700	100	30	4.3	0.430	0.013
10	700	100	40	4.3	0.323	0.017
11	700	100	50	4.3	0.258	0.022

<sup>a</sup>Energy was calculated based on the measurements of the current described in the Ref.,<sup>35</sup> where the same setup was used. Frequency of pulse repetition: 3 Hz.

PEF, pulsed electric field.

(PerkinElmer, MA).<sup>30</sup> Using the photon counting mode, a clear image can be obtained even at extremely low light levels by detecting and integrating individual photons one by one. A grayscale background image of each wound was generated, which was followed by a photon count of the same region. The entire burn photon count was quantified as relative luminescence units (RLUs) and displayed on a scale ranging from red (most intense) to blue (least intense), where luminescence showed a high degree of PA-O1:*lux* infection.<sup>29</sup> A significant linear correlation was found between bioluminescence (photon counts monitored by a low-light camera) and viable counts in this growth environment.<sup>34</sup>

Images (Fig. 1) were taken at different time points:

- D0—the immediately after-burn infection
- D1—24 h after the burn infection
- D1P—1 h after PEF treatment (25 h after the initial burn infection)
- D2—48 h after the burn infection without PEF treatment
- D2P—24 h after the PEF treatment (48 h after the initial burn infection)
- D3P—48 h after the PEF treatment (72 h after the initial burn infection)

## Histology

Skin samples were fixed in 10% formalin, embedded in paraffin, and cut into 7- $\mu$ m-thick sections that were stained with hematoxylin and eosin. The tissues were processed and stained by the Rodent Histopathology Core at Massachusetts General Hospital. Slides were evaluated by three individual investigators, including an experienced dermatopathologist, where investigators were blinded to the categories of the specimens. Color images of each entire tissue section were acquired using a NanoZoomer Digital Pathology System (NanoZoomer 2.0-HT slide scanner; Hamamatsu, Hamamatsu City, Japan).

## Quantification of cytokines, chemokines, and growth factors

Tissues were harvested at D1P and D2P (six animal samples per injury and time point), immediately flash-frozen in liquid nitrogen, and then stored at  $-80^{\circ}\text{C}$ . Subsequently, the center of the PEF-treated area was excised, and proteins were extracted in CellLytic<sup>TM</sup> MT Cell Lysis Reagent (C3228; Sigma, MO) mixed with protease inhibitor cocktail (P8340; Sigma) using a Mini-Beadbeater-1 (BioSpec, OK) with 5.5 g/cc density zirconia beads (BioSpec). Tubes with the buffer and beads were shaken four times for 15 s at 1-min intervals, after

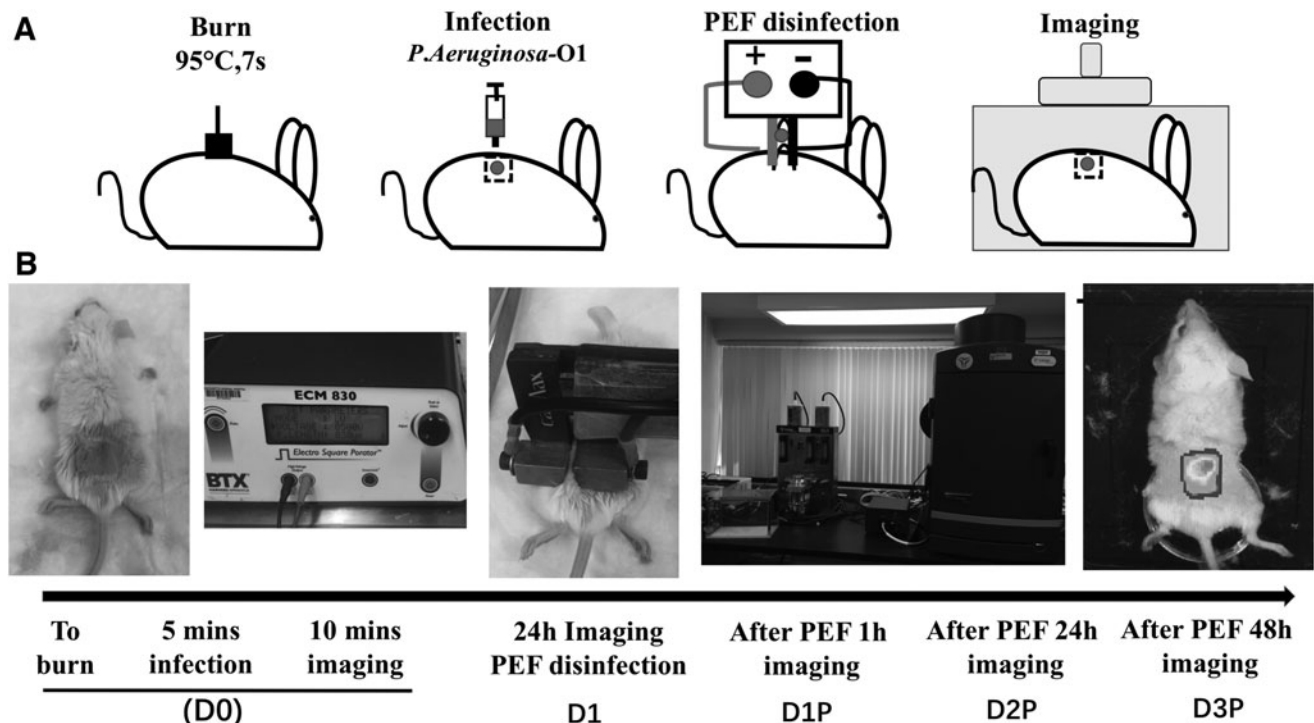


**Figure 1.** Procedure description. (A) Schematic diagram of the procedure description. (B) The actual operation of the PEF treatment procedure. PEF, pulsed electric field.

which the tubes were stored on ice. Immediately after extraction, total protein was quantified using 660 nm Protein Assay Reagent (Pierce, IL). All samples were then diluted to a single concentration, and levels of cytokines, chemokines, and growth factors were quantified using a Mouse Cytokine 32-plex Discovery Assay (Eve Technologies, Calgary, AB, Canada). After quantification, the concentration of each factor was normalized to the total protein concentration of each sample.

### Statistical analyses

Quantitative data are presented as mean  $\pm$  SE. GraphPad PRISM was used to perform *t*-test and one-way ANOVAs to evaluate differences in the immunological test results. A *p*-value of  $<0.05$  was considered significant. All experiments were replicated three times unless stated otherwise.

## RESULTS

### Optimization of PEF parameters

For PEF procedural optimization, nine different sets of PEF parameters were investigated (Table 1). All animals survived the PEF treatment. According to the bioluminescence imaging results for the PA-O1: *lux* infection load, after PEF treatment for over 3 days, group 4 (500 V, 100- $\mu$ s duration, and 200 pulses) showed the strongest effect in reducing the bacterial burden on all days except D2P, where group 10 (700 V, 40- $\mu$ s duration, and 100 pulses) showed the highest bacterial burden reduction ( $p < 0.05$ ). Group 10 (700 V, 40- $\mu$ s duration, and 100 pulses) showed no significant difference in the bacterial burden on D2P compared with that observed in the control group ( $p > 0.05$ ). Thus, the parameters used for group 4 (500 V, 100- $\mu$ s duration, 200 pulses, current  $3.1 \pm 0.4$  A,<sup>35</sup>  $0.047 \mu\text{C/s}$ , and  $0.062 \text{ C/treatment}$ ) were used in subsequent assays (Fig. 2 and Supplementary Table S1).

### Histological assessments

For histological assessments, we harvested samples at D1, D1P, D2, and D2P with 500 V, 100  $\mu$ s, and 200 pulses. In the control group (untreated infected burns), the full-thickness skin tissue showed destruction of normal skin architecture at all levels from the stratum corneum, which disappeared in most of the burned areas, down to the panniculus carnosus. The areas showed coagulative necrosis, disappearance of epidermal cells, and dermal collagen fiber degeneration at D1 (Supplementary Fig. S3): collagen bundles lost their clear outlines and interbundle spaces and were congealed together, forming a

ground substance. The elastin fibers were severely fragmented. In the subcutaneous tissue, dilated vessels and swollen endothelial tissues were observed without obvious infiltration of inflammatory cells, while subcutaneous muscles exhibited degeneration and necrosis (Fig. 3A). For mice with burn injuries and PA-O1: *lux* infection, but without PEF treatment, histological observations revealed that a large number of inflammatory cells had infiltrated into the dermis and hypodermis at D1 (Fig. 3B).

In the samples at D1P, multiple histological changes were observed, including diffuse epidermal necrosis, marked dermal thinning, endothelial compaction and focal pyknosis, inflammatory cell infiltration under the epidermis, and structural damage of sebaceous glands and hair follicles (Fig. 3C).

In the control group at D2, the wound site showed thin granulation tissue, inflammatory cell infiltration under the epidermis, and structural damage to sebaceous glands and hair follicles (Fig. 3D). In the D2 group, tissues showed significant epithelial hyperplasia, necrosis of hair follicles and sebaceous glands, and vacuole structures after cell necrosis. Furthermore, fragmented muscle fibers and multifocal areas with infiltrated inflammatory cells were also observed (Fig. 3E). In contrast, in the D2P group, squamous epithelium and obvious keratosis were observed at the wound site. Furthermore, the structure of hair follicle sebaceous glands under the epidermis was essentially intact. Collagen fibers of fibroblasts were evenly arranged, with only a few infiltrating inflammatory cells (Fig. 3F).

### Mouse immunological response to local PEF treatment of *P. aeruginosa*-infected burns.

In addition to histological evaluations, we evaluated the relative protein levels of selected cytokines and growth factors that are known to mediate wound healing (Fig. 4). Protein was extracted from skin samples of mice subjected to PEF treatment with 500 V, 100  $\mu$ s, and 200 pulses at D1P and D2P. Multiple inflammatory cytokines were significantly decreased at D1P and D2P, including interleukin (IL)-1 $\alpha$ , IL-1 $\beta$ , IL-6, IL-10, leukemia inhibitory factor (LIF), and tumor necrosis factor- $\alpha$  (TNF- $\alpha$ ). Similar changes were also observed for the chemokines, monocyte chemoattractant protein-1 (MCP-1) and macrophage inflammatory protein (MIP)-1 $\alpha$  and MIP-1 $\beta$ . Moreover, expression levels of vascular endothelial growth factor (VEGF) and several cytokines involved in immunocyte differentiation, such as

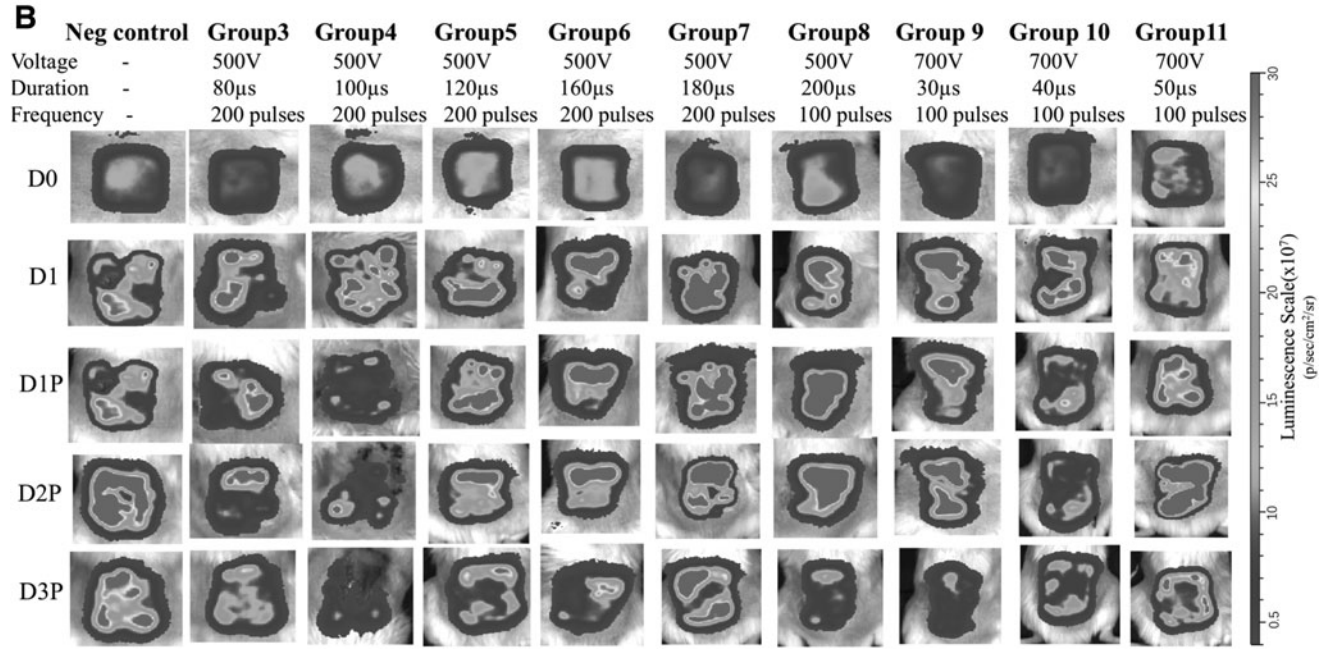
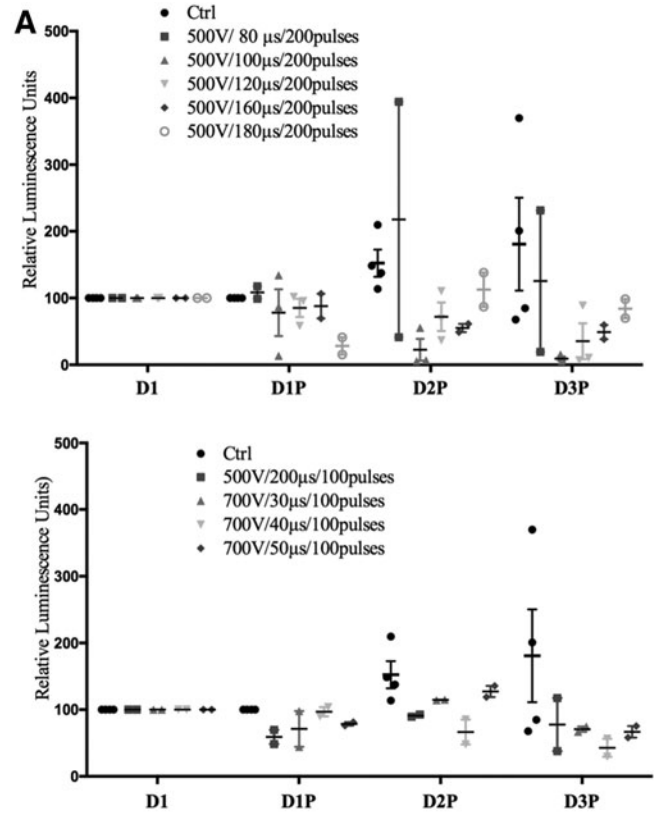


**Figure 2.** PEF optimization parameters. **(A)** Changes in luminescence for different PEF parameters over time. The parameters, 500 V, 100-µs duration, and 200 pulses, showed a significant difference compared with the control group and the other groups on D2P ( $p < 0.05$ ). **(B)** Changes in luminescence concerning all experimental parameters over time. High luminescence showed a high level of PA-O1: *lux* infection. The disinfecting effect of PEF treatment over time could be detected by the decrease in luminescence.

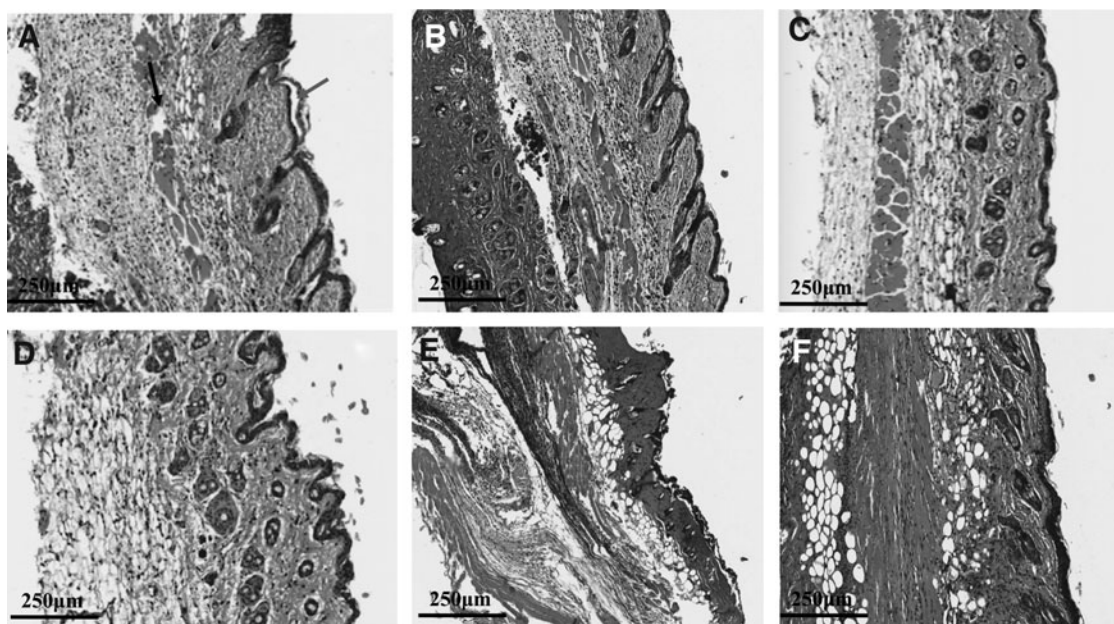


**Figure 3.** Histological results for mice with or without PEF treatment after PA-O1: *lux* infection (20 $\times$ ). (A) Negative control 24 h after burn injury without PA-O1: *lux* infection or PEF treatment. *Blue arrow*: coagulated necrotic epidermis. *Green arrow*: damaged dermal hair follicles and sebaceous glands. *Black arrow*: disordered subcutaneous muscle tissue. (B) D1 (*yellow arrow*: obvious inflammatory cell infiltration). (C) D1P. (D) Negative control 48 h after burn injury without PA-O1: *lux* infection or PEF treatment. (E) D2. (F) D2P.

macrophage colony-stimulating factor (M-CSF) and granulocyte–macrophage colony-stimulating factor (GM-CSF), were also greatly decreased after PEF treatment.

We observed lower expression of IL-1 $\alpha$  and IL-1 $\beta$  at D1P and D2P compared with D0 ( $p < 0.05$ ). IL-6 and IL-10 expression levels were significantly decreased after D2P compared with those observed in the D2 group at the same time point ( $p < 0.05$ ).

MIP-1 $\alpha$ , MIP-1 $\beta$ , MCP-1, M-CSF, LIF, and TNF- $\alpha$  showed marked reductions at D1P ( $p < 0.01$ ), whereas no differences were observed at D2P. In addition, the expression levels of VEGF and GM-CSF were greatly decreased at D1P and D2P ( $p < 0.01$ ).

Notably, expression levels of the above cytokines have been previously reported to be significantly increased in burn infection patients compared with those observed in controls and are indicated as markers of infection and inflammation progression.<sup>36</sup>

## DISCUSSION

In the present study, we investigated the disinfection effects of PEFs against *P. aeruginosa* burn infections in mice. To monitor the magnitude of the infection *in vivo*, a specific luminescent *P. aeruginosa* strain (PA-O1: *lux*) was used for quantitative

assessment of the bacterial burden of wound infections.<sup>37,38</sup> The luminescence signal from PA-O1: *lux* has been well demonstrated to indicate bacterial viability in real time.<sup>29,33</sup> Therefore, in this study, the decrease in bacterial luminescence after PEF treatment was evaluated daily to optimize the PEF parameters for maximum disinfection. Moreover, this is the first time that the response levels of cytokines and chemokines in infected burn tissues were evaluated after PEF treatment. These results provided new insights into the disinfection effect of PEF treatment of burn wounds.

The development of novel and practical concepts to prevent and treat these wound infections is the key to effective wound management.<sup>39</sup> In past decades, numerous studies have demonstrated the applications of high-voltage PEF technology in disinfection of food and contaminated water.<sup>40,41</sup> Compared with antibiotics, high-voltage PEF treatment is a noninvasive approach that precisely targets the interface of the biological membrane through electroporation, without affecting the extracellular matrix architecture.<sup>42</sup> Compared with other methods used to deliver electric fields to wounds, such as high-voltage, monophasic pulsed current energy<sup>20–22,43</sup>; low-voltage electrolysis<sup>44</sup>; or low-voltage, galvanic element-powered, wireless electroceutical dressing (WED),<sup>45–47</sup> PEF treatment uses high-voltage and high-current protocols

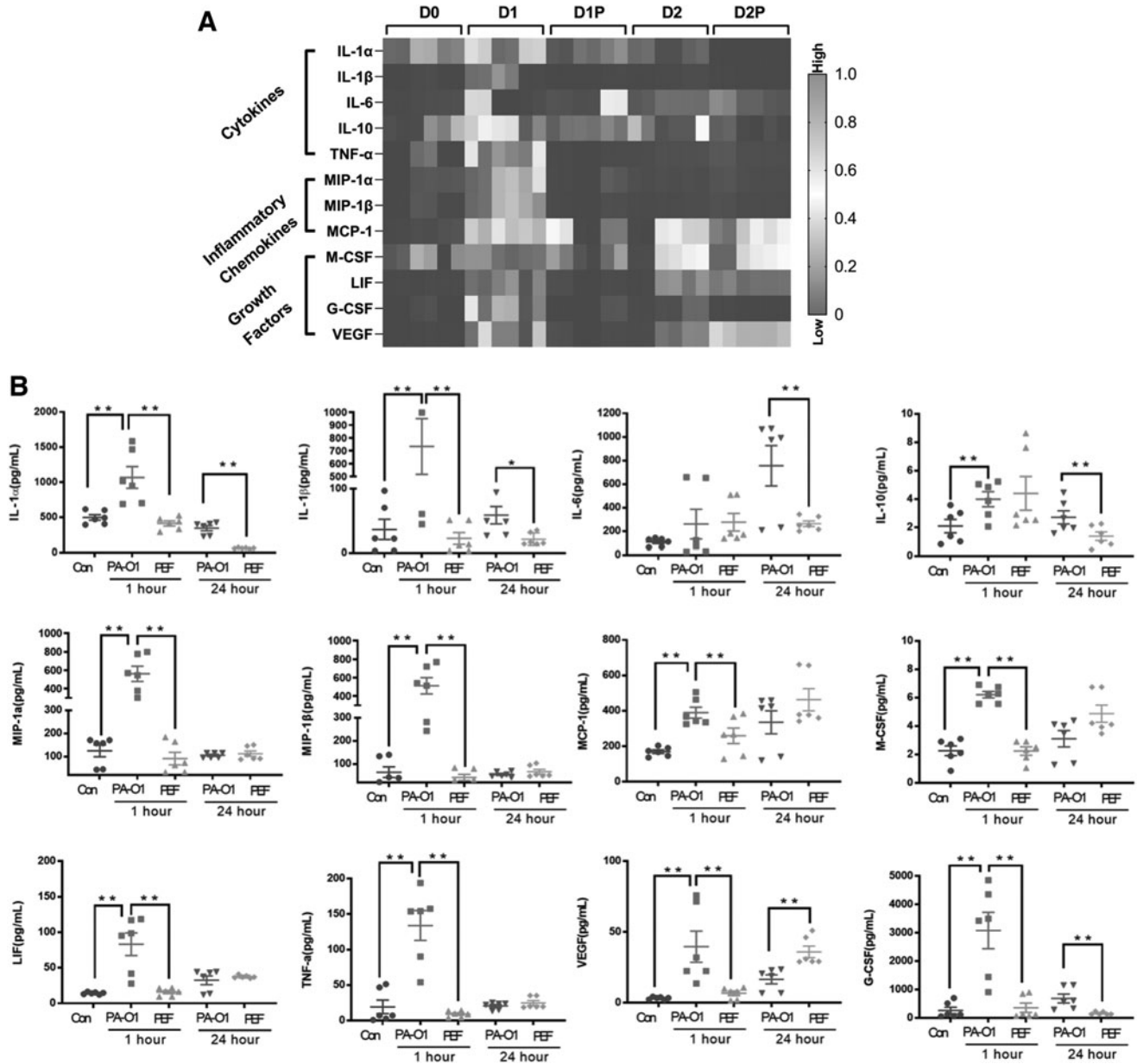


**Figure 4.** Mouse immunological response to local PEF treatment of *Pseudomonas aeruginosa*-infected burns. **(A)** Cytokine profiling of infected burn tissue after PEF treatment. **(B)** Cytokine expression in infected burn tissue after PEF treatment. We indicate with \* the comparisons between cytokine levels in the untreated and PEF-treated groups, which are significant ( $*p < 0.05$ ,  $**p < 0.01$  by *t*-test).

of short time duration, which last for seconds instead of tens of minutes. Although the exact mechanisms of interactions between electric fields and cells are not known, weak, low-voltage, low-current electric fields applied for long periods and high-voltage, short electric fields applied rapidly probably have various effects on the bacterial load in wounds. Indeed, low electric fields, such as those generated by FDA-cleared WED, were shown to host an active redox couple that is capable of reducing molecular oxygen to the superoxide anion radical, which in turn dismutates to hydrogen

peroxide. On the other hand, WED may accelerate keratinocyte migration and promote wound closure.<sup>48</sup> A combination of hydrogen peroxide and superoxide anion radicals in the wound environment for days, as provided by WED, contributes to both direct inactivation of bacteria and stimulation of local neutrophils.<sup>49</sup> Patterned electroceutical dressing is safe and can potentially be used to treat deeply infected wounds.<sup>50</sup> Low electric fields were also suggested to trigger electrolysis for generation of other disinfecting compounds such as hypochlorous acid.<sup>44</sup> A high-voltage PEF, however, was



shown to directly modify the bacterial cell wall<sup>51</sup> and cell membrane permeabilization through electroporation. Although a high-voltage PEF could also lead to electrochemical reactions in the treated media,<sup>52</sup> they could be reduced by shortening the pulse duration. Interestingly, previous works suggested devices (fabrics) that combine electroporation with hydrogen peroxide generation,<sup>53</sup> thus harvesting the advantage of potential mechanisms of both types of electric field treatments for wound care.

In our previous studies, we demonstrated that PEF treatment exhibited *in vitro* antibacterial effects on gel surfaces,<sup>35,54</sup> suggesting the potential use of PEF treatment in wound healing *in vivo*. In this study, we observed that the treatment of burn wounds with PEFs resulted in ~78% and 91% inhibition of bacteria at 2 and 3 days after treatment, respectively. Although previous studies using a murine model suggested that increasing the voltage of the PEF may provide better bacterial load reduction 3 h after the treatment,<sup>55</sup> after comparing the antibacterial effects of the PEF with different parameters for 3 days in this study, we concluded that increasing the voltage or pulse duration in the tested ranges did not significantly increase the disinfection efficacy (Supplementary Table S1). Therefore, for safety, a lower voltage (500 V) and moderate pulse duration (200 pulses and 100  $\mu$ s) were selected as the optimal parameters in our experiment. Nevertheless, the future application of PEFs to clinically relevant wound sizes requires the development of electrodes with large surfaces or arrays of multiple electrodes. Several electrode arrays and flexible surface electrodes for use in disinfection have been reported for other electroporation treatments.<sup>56–58</sup>

The disinfection potential of the PEF treatment depends on the locally induced transmembrane potential of bacterial cells,<sup>59</sup> which depends strongly on tissue morphology and electrical conductivity.<sup>60</sup> Thus, the effective penetration for PEF disinfection from external electrodes to the wound depends on the specific configuration of electrodes,<sup>58</sup> such as the geometry, size, number, and distance between the electrodes, as well as the skin temperature, humidity state, and other factors. To estimate the local electric field strength inside complex tissues, such as the skin and burns, using an infected burn rat model, we have previously published a numerical model for electric field distribution and thermal heating.<sup>35,55</sup>

In addition, the effect of the PEF treatment can be immediate, involving the direct killing of cells by electric fields, or postponed due to delayed apo-

ptosis or subsequent pathogen elimination by an activated immune response.<sup>61</sup> The efficiency of PEF treatment also depends on possible wound reinfection from untreated skin or the environment as well as the immunological condition of the host.<sup>55</sup> Hosts that recover faster could fight the infection better than those whose condition does not change or worsens,<sup>46</sup> and the acquired immunity aids in preventing new and aggressive infections.<sup>62,63</sup> Nevertheless, the actual long-term outcomes of the disinfection of healing burn wounds by PEF treatment were not assessed in this study and require further detailed analysis. Compared with mammalian cells, bacteria are less sensitive to electroporation due to their cell size, cell wall, and internal structure.<sup>51</sup> Therefore, the PEF parameters required to inactivate bacteria may cause tissue ablation or injury at the treatment site.<sup>64</sup> Our previous work on PEF treatment of normal tissue and noninfected burn wounds showed that high-voltage PEF ablation leads to complete normal tissue regeneration and promotes the healing of burn wounds with smaller scars.<sup>31,65,66</sup>

The extent of inflammation is related to the depth and extent of the burn as deeper burns lead to higher levels of circulating cytokines.<sup>67</sup> It has been reported that at 2 or 3 days after burn infection, the inflammatory response transitions into a proliferative phase, in which fibroblasts from the deep dermis slowly proliferate, produce inflammatory cytokines (including TGF- $\beta$ ), and synthesize proteoglycans and procollagen to create granulation tissue.<sup>68</sup> According to our histological results, direct cellular damage occurs in the electrode-covered central ablation zone after the PEF treatment was delivered, which may initiate an indirect anti-inflammatory response within the infection area, corroborating our previous studies on the impacts of PEFs on the rodent normal skin.<sup>28,31,69</sup>

Burn wounds are characterized by persistently high numbers of neutrophils that express proinflammatory cytokines, including TNF- $\alpha$ , IL-1 $\beta$ , and IL-6.<sup>70</sup> To observe whether PEF treatment affected the inflammation microenvironment within the burn area, we measured the profiles of 32 cytokines and chemokines in wound tissue. PEF treatment significantly attenuated the levels of MIP-1 $\alpha$  and MIP-1 $\beta$  at the injection site, indicating the possibility of less collagen synthesis in these wounds compared with those in the untreated control mice. Moreover, PEF treatment also resulted in decreased levels of IL-6, MCP-1, TNF- $\alpha$ , and VEGF. It is well known that production of IL-6 is increased

after a burn injury, and higher levels of both IL-6 and its receptors are closely correlated with the secretion of VEGF and TNF- $\alpha$  activity.<sup>71,72</sup> Thus, our findings suggested that PEF treatment suppresses IL-1 $\beta$ , TNF- $\alpha$ , and IL-6 levels and prevents the subsequent release of other cytokines and chemokines in response to injury. These results are in agreement with previous reports showing that the IL-6 family mediates the immune responses in inflammatory diseases, which are viewed as major therapeutic targets for clinical intervention.<sup>73</sup>

VEGF stimulates wound healing through multiple mechanisms, including collagen deposition, angiogenesis, and epithelialization.<sup>74</sup> In our results, VEGF expression decreased at the beginning and then increased at D2P. According to a study by Brem and Folkman, new vessels appear 3 days after wounding in angiogenesis.<sup>75</sup> PEF treatment may improve tissue perfusion as early as 2 days after treatment by promoting angiogenesis. In addition, MCP-1, MCF, and G-CSF are important chemokines for severe inflammation.<sup>76</sup> IL-10 is a cytokine with potent anti-inflammatory properties and plays a key role in limiting host immune responses to pathogens.<sup>77</sup> PEF treatment significantly attenuated the increases in those chemokines, suggesting that PEF may modulate the inflammatory response. In summary, PEF treatment may serve as an alternative therapeutic option for burn infections by preventing inflammation.

One of the limitations of this study is the lack of precise measurement of the therapeutic PEF penetration depth.<sup>78</sup> An additional limitation is primarily related to biological variability in the response of each mouse to bacteria and the systematic error in measuring RLU signals. To perform equivalent comparisons, the signal of each animal was normalized to the percentage of RLU compared with that observed on D1. To avoid these drawbacks, a large number of replicate animals are needed to confirm our findings in a future study. An additional limitation of the study is the lack of a clear mechanism of high-voltage PEF action on bacterial cells and the treated wound bed. The optimized protocol, 500 V, 100  $\mu$ s, and 200 pulses delivered at 3 Hz, could lead to multiple simultaneous events, such as direct bacterial and host cell killing, bacterial and host cell injury through electroporation, and various electrochemical reactions, generated at the electrodes and the cell surface,<sup>79</sup> which affect both bacteria and host cells. In addition, the consequences of high-voltage PEF appli-

## KEY FINDINGS

- The combination of 500 V, 100  $\mu$ s, and 200 pulses delivered at 3 Hz through two plate electrodes positioned 1 mm apart led to the best *P. aeruginosa* disinfection efficacy up to 3 days after the burn injury.
- PEF-treated wounds showed less histological inflammation than the untreated controls.
- PEF treatment leads to long-term disinfection of burn wounds.

cation on infection wound rescue and skin barrier restoration are missing in this study and are the subject of future work.

In summary, PEF treatment is a potentially effective, physical therapy approach for localized infections. Furthermore, we demonstrated that PEF treatment reduces the bacterial load and mediates inflammatory responses in burn infections. However, the mechanisms underlying the PEF toward antimicrobial treatment, host immune responses, and skin barrier restoration need further study.

## INNOVATION

Previous studies showed immediate inactivation of bacteria in wounds upon PEF treatment. The results of this study suggest that PEF effects are not only immediate but long-term reduction of the infection load is also observed. Thus, the development of effective PEF disinfection therapy could significantly contribute to clinical management of burn injury patients.

## ACKNOWLEDGMENTS AND FUNDING SOURCES

This study was supported by the United States–Israel Binational Science Foundation, number 2017129. The funders had no role in the study design, data collection and analysis, decision to publish, or preparation of the manuscript. The authors acknowledge the Shriners Hospital for Children (Grant number 85125-BOS-19) and the NJ Commission on Spinal Cord Research for partial support of this work.

## AUTHOR DISCLOSURE AND GHOSTWRITING

No competing financial interests exist. The authors listed expressly wrote the content of this article. No ghostwriters were used to write this article.

## ABOUT THE AUTHORS

**Mengjie Wu, DMD, PhD**, is an Associate Professor at the Medical School in Zhejiang Uni-

versity. She worked as a research fellow in Massachusetts General Hospital at HMS. Her major research focuses on anti-inflammation therapy on wound healing and tissue engineering. **Andrey Ethan Rubin, MSc**, is a PhD Student at the PSEES. He is a biologist working in the interface of sciences, technology, and engineering to advance human health. **Tianhong Dai, PhD**, is an Assistant Professor at HMS. His research interests are centered around using light-based antimicrobial therapeutics for antibiotic-resistant infections. **Osman Berk Usta, PhD** is an Assistant Professor of Surgery at HMS, His work lies at the intersection between micro-tissue engineering, biopreservation, and computational modeling. **Alexander Golberg, PhD** is an Associate Professor at the

PSEES. His research interests are in the development of new technologies for human health with a specific emphasis on burns and wound healing. **Martin Yarmush, MD, PhD**, is a Professor of Biomedical Engineering at Rutgers University and Director of the Center for Engineering in Medicine at HMS. His research is in the fields of metabolic engineering, wound healing and technology development for critical medical applications.

## SUPPLEMENTARY MATERIAL

Supplementary Figure S1  
 Supplementary Figure S2  
 Supplementary Figure S3  
 Supplementary Table S1

## REFERENCES

- American Burn Association. Burn Incidence Fact Sheet. Chicago, IL: American Burn Association, 2002.
- Evarts B. NFPA's "Fire Loss in the United States During 2017". Quincy, MA: National Fire Protection Association, 2018.
- Sheridan RL. Burns. A Practical Approach to Immediate Treatment and Long-Term Care. London: Manson Publishing, 2012.
- Kraft R, Herndon DN, Finnerty CC, Cox RA, Song J, Jeschke MG. Predictive value of il-8 for sepsis and severe infections after burn injury: a clinical study. *Shock* 2015;43:222–227.
- Devrim I, Kara A, Duzgol M, et al. Burn-associated bloodstream infections in pediatric burn patients: time distribution of etiologic agents. *Burns* 2017; 43:144–148.
- El Zowalaty ME, Al Thani AA, Webster TJ, et al. *Pseudomonas aeruginosa*: arsenal of resistance mechanisms, decades of changing resistance profiles, and future antimicrobial therapies. *Future Microbiol* 2015;10:1683–1706.
- Eshabani HK, Kashani PP, Ghanaatpisheh F. Frequency of *Pseudomonas aeruginosa* serotypes in burn wound infections and their resistance to antibiotics. *Burns* 2002;28:340–348.
- Parcell BJ, Oravcova K, Pinheiro M, et al. *Pseudomonas aeruginosa* intensive care unit outbreak: winnowing of transmissions with molecular and genomic typing. *J Hosp Infect* 2018;98:282–288.
- Herndon DN, Spies M. Modern burn care. *Semin Pediatr Surg* 2001;10:28–31.
- Karnes JB. Skin infections and outpatient burn management: outpatient burn management. *FP Essent* 2020;489:27–31.
- Zampar EF, Anami EHT, Kerbauy G, et al. Infectious complications in adult burn patients and antimicrobial resistance pattern of microorganisms isolated. *Ann Burns Fire Disasters* 2017;30: 281–285.
- Bassetti M, Vena A, Croxatto A, Righi E, Guery B. How to manage *Pseudomonas aeruginosa* infections. *Drugs Context* 2018;7:212527.
- Oncul O, Oksuz S, Acar A, et al. Nosocomial infection characteristics in a burn intensive care unit: analysis of an eleven-year active surveillance. *Burns* 2014;40:835–841.
- Yoshino Y, Ohtsuka M, Kawaguchi M, et al. The wound/burn guidelines—6: guidelines for the management of burns. *J Dermatol* 2016;43:989–1010.
- Bush K, Courvalin P, Dantas G, et al. Tackling antibiotic resistance. *Nat Rev Microbiol* 2011;9: 894–896.
- Yarmush ML, Golberg A, Sersa G, Kotnik T, Miklavcic D. Electroporation-based technologies for medicine: principles, applications, and challenges. *Annu Rev Biomed Eng* 2014;16:295–320.
- Rubinsky B. Irreversible Electroporation. Verlag Berlin Heiderberg: Springer, 2010.
- Golberg A, Yarmush ML. Nonthermal irreversible electroporation: fundamentals, applications, and challenges. *IEEE Trans Biomed Eng* 2013;60:707–714.
- Golberg A, Rae CS, Rubinsky B. Listeria monocytogenes cell wall constituents exert a charge effect on electroporation threshold. *Biochim Biophys Acta* 2012;1818:689–694.
- Girgis B, Duarte JA. High voltage monophasic pulsed current (HVMP) for stage II-IV pressure ulcer healing. A systematic review and meta-analysis. *J Tissue Viability* 2018;27:274–284.
- Kloth LC. Electrical stimulation technologies for wound healing. *Adv Wound Care (New Rochelle)* 2014;3:81–90.
- Polak A, Kucio C, Kloth LC, et al. A randomized, controlled clinical study to assess the effect of anodal and cathodal electrical stimulation on periwound skin blood flow and pressure ulcer size reduction in persons with neurological injuries. *Ostomy Wound Manage* 2018;64:10–29.
- Pucihar G, Krmelj J, Rebersek M, Napotnik TB, Miklavcic D. Equivalent pulse parameters for electroporation. *IEEE Trans Biomed Eng* 2011;58: 3279–3288.
- Rems L MD. Tutorial: electroporation of cells in complex materials and tissue. *J Appl Phys* 2016; 119. DOI: 10.1063/1.4949264.
- Jones SA, Jenkins BJ. Recent insights into targeting the IL-6 cytokine family in inflammatory diseases and cancer. *Nat Rev Immunol* 2018;18: 773–789.
- Jeschke MG, Norbury WB, Finnerty CC, et al. Age differences in inflammatory and hypermetabolic postburn responses. *Pediatrics* 2008;121: 497–507.

27. Khan SI, Blumrosen G, Vecchio D, et al. Eradication of multidrug-resistant *Pseudomonas* biofilm with pulsed electric fields. *Biotechnol Bioeng* 2016;113:643–650.
28. Golberg A, Khan S, Belov V, et al. Skin rejuvenation with non-invasive pulsed electric fields. *Sci Rep* 2015;5:10187.
29. Leanse LG, Harrington OD, Fang Y, Ahmed I, Goh XS, Dai T. Evaluating the potential for resistance development to antimicrobial blue light (at 405 nm) in Gram-negative bacteria: in vitro and in vivo studies. *Front Microbiol* 2018;9:2403.
30. Dai T, Gupta A, Huang YY, et al. Blue light rescues mice from potentially fatal *Pseudomonas aeruginosa* burn infection: efficacy, safety, and mechanism of action. *Antimicrob Agents Chemother* 2013;57:1238–1245.
31. Golberg A, Villiger M, Felix Broelsch G, et al. Skin regeneration with all accessory organs following ablation with irreversible electroporation. *J Tissue Eng Regen Med* 2018;12:98–113.
32. Rubin AE, Usta OB, Schloss R, Yarmush M, Golberg A. Selective inactivation of *Pseudomonas aeruginosa* and *Staphylococcus epidermidis* with pulsed electric fields and antibiotics. *Adv Wound Care (New Rochelle)* 2019;8:136–148.
33. Leanse LG, Dong PT, Goh XS, et al. Quinine enhances photo-inactivation of Gram-negative bacteria. *J Infect Dis* 2020;221:618–626.
34. Thorn RM, Nelson SM, Greenman J. Use of a bioluminescent *Pseudomonas aeruginosa* strain within an in vitro microbiological system, as a model of wound infection, to assess the antimicrobial efficacy of wound dressings by monitoring light production. *Antimicrob Agents Chemother* 2007;51:3217–3224.
35. Golberg A, Broelsch GF, Vecchio D, et al. Eradication of multidrug-resistant *A. baumannii* in burn wounds by antiseptic pulsed electric field. *Technology (Singap World Sci)* 2014;2:153–160.
36. Farina JA, Jr., Rosique MJ, Rosique RG. Curbing inflammation in burn patients. *Int J Inflamm* 2013; 2013:715645.
37. de Vries CR, Sweere JM, Ishak H, et al. A delayed inoculation model of chronic *Pseudomonas aeruginosa* wound infection. *J Vis Exp* 2020. [Epub ahead of print]; DOI: 10.3791/60599.
38. Sweere JM, Ishak H, Sunkari V, et al. The immune response to chronic *Pseudomonas aeruginosa* wound infection in immunocompetent mice. *Adv Wound Care (New Rochelle)* 2020;9:35–47.
39. Sen CK. Human wounds and its burden: an updated compendium of estimates. *Adv Wound Care (New Rochelle)* 2019;8:39–48.
40. Otunola A, El-Hag A, Jayaram S, Anderson WA. Effectiveness of pulsed electric fields in controlling microbial growth in milk. *Int J Food Eng* 2008;4:1–14.
41. Barbosa-Cánovas GV, Gongora-Nieto MM, Pothakamury UR, Swanson BG. Preservation of Foods with Pulsed Electric Fields. London: Academic Press Ltd., 1999.
42. Alhabash S, McAlister AR, Hagerstrom A, Quilliam ET, Rifon NJ, Richards JI. Between likes and shares: effects of emotional appeal and virality on the persuasiveness of antibullying messages on Facebook. *Cyberpsychol Behav Soc Netw* 2013; 16:175–182.
43. Iazzo PA. Engineering in Medicine: Advances and Challenges. London: Elsevier Science, 2018.
44. Rubinsky L, Patrick B, Mikus P, Rubinsky B. Germicide wound pad with active, in situ, electrolytically produced hypochlorous acid. *Biomed Microdevices* 2016;18:26.
45. Barki KG, Das A, Dixith S, et al. Electric field based dressing disrupts mixed-species bacterial biofilm infection and restores functional wound healing. *Ann Surg* 2019;269:756–766.
46. Banerjee J, Das Ghatak P, Roy S, et al. Improvement of human keratinocyte migration by a redox active bioelectric dressing. *PLoS One* 2014;9:e89239.
47. Ghatak PD, Schlanger R, Ganesh K, et al. A wireless electroceutical dressing lowers cost of negative pressure wound therapy. *Adv Wound Care (New Rochelle)* 2015;4:302–311.
48. Banerjee J, Das Ghatak P, Roy S, et al. Silver-zinc redox-coupled electroceutical wound dressing disrupts bacterial biofilm. *PLoS One* 2015;10: e0119531.
49. Bender HS, Chickering WR. Superoxide, superoxide dismutase and the respiratory burst. *Vet Clin Pathol* 1983;12:7–14.
50. Roy S, Prakash S, Mathew-Steiner SS, et al. Disposable patterned electroceutical dressing (PED-10) is safe for treatment of open clinical chronic wounds. *Adv Wound Care (New Rochelle)* 2019;8:149–159.
51. Pillet F, Formosa-Dague C, Baaziz H, Dague E, Rols MP. Cell wall as a target for bacteria inactivation by pulsed electric fields. *Sci Rep* 2016;6:19778.
52. Chafai DE, Mehle A, Tilmatine A, Maouche B, Miklavcic D. Assessment of the electrochemical effects of pulsed electric fields in a biological cell suspension. *Bioelectrochemistry* 2015;106:249–257.
53. Che-Min C, Ke Y-Y, Chou T-M, et al. Self-powered active antibacterial clothing through hybrid effects of nanowire-enhanced electric field electroporation and controllable hydrogen peroxide generation. *Nano Energy* 2018;53:1–10.
54. Rubin AE, Levkov K, Usta OB, Yarmush M, Golberg A. IGBT-based pulsed electric fields generator for disinfection: design and in vitro studies on *Pseudomonas aeruginosa*. *Ann Biomed Eng* 2019;47: 1314–1325.
55. Golberg A, Broelsch GF, Vecchio D, et al. Pulsed electric fields for burn wound disinfection in a murine model. *J Burn Care Res* 2015;36:7–13.
56. Ongaro A, Campana LG, De Mattei M, et al. Evaluation of the electroporation efficiency of a grid electrode for electrochemotherapy: from numerical model to in vitro tests. *Technol Cancer Res Treat* 2016;15:296–307.
57. Wei Z, Huang Y, Zhao D, Hu Z, Li Z, Liang Z. A pliable electroporation patch (ep-Patch) for efficient delivery of nucleic acid molecules into animal tissues with irregular surface shapes. *Sci Rep* 2015;5:7618.
58. Golberg A, Rubinsky B. Towards electroporation based treatment planning considering electric field induced muscle contractions. *Technol Cancer Res Treat* 2012;11:189–201.
59. Kotnik T, Pucihar G, Miklavcic D. Induced transmembrane voltage and its correlation with electroporation-mediated molecular transport. *J Membr Biol* 2010;236:3–13.
60. Golberg A, Bruinsma BG, Uygun BE, Yarmush ML. Tissue heterogeneity in structure and conductivity contribute to cell survival during irreversible electroporation ablation by “electric field sinks.” *Sci Rep* 2015;5:8485.
61. Zhang Y, Lyu C, Liu Y, Lv Y, Chang TT, Rubinsky B. Molecular and histological study on the effects of non-thermal irreversible electroporation on the liver. *Biochem Biophys Res Commun* 2018;500: 665–670.
62. Maurice NM, Bedi B, Sadikot RT. *Pseudomonas aeruginosa* biofilms: host response and clinical implications in lung infections. *Am J Respir Cell Mol Biol* 2018;58:428–439.
63. Jensen PO, Givskov M, Bjarnsholt T, Moser C. The immune system vs. *Pseudomonas aeruginosa* biofilms. *FEMS Immunol Med Microbiol* 2010;59: 292–305.
64. Baah-Dwomoh A, Rolong A, Gatenholm P, Davalos RV. The feasibility of using irreversible electroporation to introduce pores in bacterial cellulose scaffolds for tissue engineering. *Appl Microbiol Biotechnol* 2015;99:4785–4794.
65. Kravez E, Villiger M, Bouma B, Yarmush M, Yakhini Z, Golberg A. Prediction of scar size in rats six months after burns based on early post-injury polarization-sensitive optical frequency domain imaging. *Front Physiol* 2017;8:967.
66. Golberg A, Villiger M, Khan S, et al. Preventing scars after injury with partial irreversible electroporation. *J Invest Dermatol* 2016;136:2297–2304.
67. Sakalliglu AE, Basaran O, Karakayali H, et al. Interactions of systemic immune response and local wound healing in different burn depths: an experimental study on rats. *J Burn Care Res* 2006; 27:357–366.
68. Aguilera-Saez J, Munoz P, Serracanta J, Monte A, Barret JP. Extracorporeal shock wave therapy role in the treatment of burn patients. A systematic literature review. *Burns* 2019. [Epub ahead of print]; DOI: 10.1016/j.burns.2019.07.023.
69. Li X, Saeidi N, Villiger M, et al. Rejuvenation of aged rat skin with pulsed electric fields. *J Tissue Eng Regen Med* 2018;12:2309–2318.
70. Serra MB, Barroso WA, da Silva NN, et al. From inflammation to current and alternative therapies involved in wound healing. *Int J Inflamm* 2017;2017: 3406215.

71. Schwacha MG. Macrophages and post-burn immune dysfunction. *Burns* 2003;29:1–14.
72. Feurino LW, Zhang Y, Bharadwaj U, et al. IL-6 stimulates Th2 type cytokine secretion and upregulates VEGF and NRP-1 expression in pancreatic cancer cells. *Cancer Biol Ther* 2007;6:1096–1100.
73. Hunter CA, Jones SA. IL-6 as a keystone cytokine in health and disease. *Nat Immunol* 2015;16:448–457.
74. Bao P, Kodra A, Tomic-Canic M, Golinko MS, Ehrlich HP, Brem H. The role of vascular endothelial growth factor in wound healing. *J Surg Res* 2009;153:347–358.
75. Brem H, Folkman J. *Angiogenesis and Basic Fibroblast Growth Factor During Wound Healing*. Rosemont: American Academy of Orthopedic Surgeons, 1994.
76. Gupta M, Chaturvedi R, Jain A. Role of monocyte chemoattractant protein-1 (MCP-1) as an immune-diagnostic biomarker in the pathogenesis of chronic periodontal disease. *Cytokine* 2013;61:892–897.
77. Iyer SS, Cheng G. Role of interleukin 10 transcriptional regulation in inflammation and autoimmune disease. *Crit Rev Immunol* 2012;32:23–63.
78. Novickij V, Lastauskiene E, Staigvila G, et al. Low concentrations of acetic and formic acids enhance the inactivation of *Staphylococcus aureus* and *Pseudomonas aeruginosa* with pulsed electric fields. *BMC Microbiol* 2019;19:73.
79. Teissie J. Involvement of reactive oxygen species in membrane electroporation. In: Miklavcic D, ed. *Handbook of Electroporation*. Cham: Springer, 2017:1–15.

### Abbreviations and Acronyms

GM-CSF	= granulocyte-macrophage colony-stimulating factor
i.p.	= intraperitoneal
IL	= interleukin
LIF	= leukemia inhibitory factor
MCP-1	= monocyte chemoattractant protein-1
M-CSF	= macrophage colony-stimulating factor
MIP	= macrophage inflammatory protein
PBS	= phosphate-buffered saline
PEF	= pulsed electric field
RLUs	= relative luminescence units
TNF- $\alpha$	= tumor necrosis factor-alpha
VEGF	= vascular endothelial growth factor
WED	= wireless electroceutical dressing